Journal of Physics D: Applied Physics

PAPER

Observation of band gap fluctuations and carrier localization in $Cu_2CdGeSe_4$

To cite this article: Jüri Krustok *et al* 2019 *J. Phys. D: Appl. Phys.* **52** 285102

IOP Publishing Journal of Physics D: Applied Physics
J. Phys. D: Appl. Phys. **52** (2019) 285102 (7pp) https://doi.org/10.1088/1361-6463/ab1afd

Observation of band gap fluctuations and carrier localization in $Cu_2CdGeSe_4$

Jüri Krustok[1,2], Taavi Raadik[2], Reelika Kaupmees[2], Maarja Grossberg[2], Marit Kauk-Kuusik[2], Kristi Timmo[2] and Arvo Mere[1,2]

[1] Division of Physics, Tallinn University of Technology, Ehitajate tee 5, 19086 Tallinn, Estonia
[2] Department of Materials and Environmental Technology, Tallinn University of Technology, Ehitajate tee 5, 19086 Tallinn, Estonia

E-mail: Juri.Krustok@ttu.ee

Received 28 January 2019, revised 10 April 2019
Accepted for publication 18 April 2019
Published 8 May 2019

Abstract

Excitation power and temperature dependences of the steady-state photoluminescence (PL) spectra are studied in polycrystalline $Cu_2CdGeSe_4$ (CCGSe) containing a mixture of orthorhombic and tetragonal phases. The low-temperature excitation power dependences of the PL peak shape with a peak position at about 1.17 eV indicate a state filling effect. Reflectivity measurements revealed band gap energies 1.257 eV and 1.223 eV at 10 K and 300 K, respectively. The temperature dependences of the peak energy and linewidth showed a 'S-shaped' and 'V-shaped' behavior, respectively, and are well explained by the localized carriers model where band gap fluctuations play a crucial role. The asymmetric PL band shape analysis indicates the presence of hot carriers having a temperature about 75 K higher than the lattice temperature. It is shown that the low-temperature PL emission is due to recombination of localized electrons with holes captured by the deep acceptor defect Cu_{Cd} with a depth $E_A = 80$ meV.

Keywords: $Cu_2CdGeSe_4$, photoluminescence, band gap fluctuations, hot carriers, localized states

(Some figures may appear in colour only in the online journal)

1. Introduction

The earth abundant kesterites $Cu_2ZnSn(S,Se)_4$ (CZTSSe) have gained much attention in materials research community for solar energy applications, but the record efficiency of CZTSSe based cells is still only 12.6% [1]. This low efficiency and lack of progress for several years for CZTSSe has motivated research on other quaternary copper chalcogenides with suitable band gap energy for solar cell absorber. Among them, the $Cu_2CdGeSe_4$ (CCGSe) compound is less studied, although having a p-type conductivity and very promising properties including a band gap energy of about 1.14–1.29 eV [2, 3, 4]. CCGSe has two crystal structure modifications: a stannite tetragonal structure with a I-42m space group (t-CCGSe) and an orthorhombic structure with a Pmn21 space group (o-CCGSe) [5]. The presence of an orthorhombic structure in CCGSe is somewhat different from CZTSSe compounds, where the kesterite structure dominates. The orthorhombic crystal structure is prevailing at higher temperatures ($T > 605$ °C) while a tetragonal crystal structure is obtained at lower ($T < 605$ °C) temperatures [2, 6]. The band gap energy values determined from external quantum efficiency measurements were 1.27 eV for o-CZTSSe and 1.14 eV for t-CZTSSe crystals [4]. A detailed low-temperature photoluminescence (PL) study of CCGSe crystals revealed different dominating radiative recombination mechanisms for orthorhombic and tetragonal CCGSe [7]. It is known that almost all quaternary copper chalcogenides show very high ($N > 10^{19}$ cm^{-3}) concentration of various intrinsic defects [8]. In ternaries, it is more or less possible to control the defect structure while in quaternary chalcogenides the situation seems to be more complicated. It is known that the high concentration of charged defects generate potential fluctuations and, as a result, tails in the density of states (DOS) of the conduction and valence bands of semiconductors [9]. At the same time, the structural or the

compositional inhomogeneity causes spatial fluctuations of the band gap energy [10]. In CZTSSe it is known that due to the difference of Cu–Zn ordering ratio in the kesterite lattice the band gap energy can vary about 100–200 meV [11]. This kind of compositional inhomogeneity could be a source for band gap fluctuations. Both, electrostatic and band gap fluctuations create potential wells where carriers can localize. Consequently, new recombination processes can be expected in these disordered chalcogenides. The theoretical study of photoluminescence properties in semiconductors with spatial potential fluctuations has been published by Levanyuk *et al* [9]. It suggests the characteristic asymmetric shape of corresponding PL bands and their strong (>10 meV per decade) blueshift with increasing excitation intensity. At the same time, less is known about band gap fluctuations and related recombination processes in chalcogenides. Band gap fluctuations can give rise to the carrier localization that is very common in disordered systems and can be detected in quantum wells, quantum dots or different semiconductor alloys [12]. The recombination processes related to carrier localization were theoretically studied by Li *et al* [13]. It was shown that the 'S-shaped' temperature dependence of the PL peak position and a reduction of the linewidth with increasing temperature are common features for recombination processes involving localized carriers. While both fluctuations (potential and band gap) share quite similar dependencies of PL bands ('S-shaped' temperature dependence of the PL peak position, asymmetrical PL band shape), there are differences that would allow to identify different recombination processes. Different band gap energies of orthorhombic and tetragonal CCGSe can be used to study carrier localization in this compound. Thus, in the present paper, we studied band gap fluctuations by using a mixture of orthorhombic and tetragonal structures in CCGSe. The experimental temperature and laser power dependencies of the photoluminescence band in CCGSe are presented. We show that all these dependencies can be explained by assuming electrons localization in potential wells created by band gap fluctuations.

2. Experimental

$Cu_2CdGeSe_4$ polycrystalline powder was synthesized from $CuSe_{0.993}$ (5N), CdSe (4N), GeSe (5N) binary compounds and elemental Se (5N) by solid-state reaction in sealed evacuated quartz ampoules. All precursors for $Cu_2CdGeSe_4$ synthesis were grounded in an agate mortar in stoichiometric composition. After mixing and grounding of precursors, the mixture was poured into a quartz ampoule, degassed under dynamic vacuum, sealed, and annealed isothermally at 900 °C for 7 h. Then, the temperature was lowered to 750 °C. To obtain a complete homogenization the mixture was kept at 750 °C for 120 h. After annealing at 750 °C, ampoules were cooled down with furnace (cooling rate of about 3 °C min^{-1}) to room temperature.

The $Cu_2CdGeSe_4$ single crystals for reflectivity measurements were grown via chemical vapor transport using iodine as a transport agent. Previously synthesized polycrystalline powder was mixed together with 4N purity CuI (5 mg of iodine per cm^3) and sealed in an evacuated quartz ampoule. The sealed ampoule was placed in a two-zone horizontal furnace. Both temperature zones were heated up to 600 °C with the heating rate of 2 °C min^{-1} and maintained at this temperature for 24 h. After that the temperatures at source and growth zones were raised up to 750 and 650 °C with the heating rate of 2 °C min^{-1}, respectively. Crystal growth process took place at these temperature regimes for two weeks. After this, both zones were cooled down to room temperature (RT) with the cooling rate of 3 °C min^{-1}. It is obvious that the ratio of orthorhombic and tetragonal structures depends on the cooling rate of the material and in order to get a mixture of both structures rather slow cooling rate was used. The bulk elemental composition of samples was analyzed by energy dispersive x-ray spectroscopy (EDX) on HR-SEM Zeiss Merlin equipped with Bruker EDX-XFlash6/30 detector with an accelerating voltage of 20 kV. These studies showed that both samples were Cu-poor (Cu 21.2, Cd 17.0, Ge 12.1 and Se 49.7 at.%) with [Cu]/[Cd + Ge] = 0.73.

The structural investigation of the CCGSe polycrystalline powder was carried out by x-ray diffraction (XRD) using a Rigaku Ultima IV diffractometer with monochromatic Cu Kα1 radiation ($\lambda = 1.5406$ Å) at 40 kV and 40 mA operating with the silicon strip detector D/teX Ultra. All samples were studied in the 2θ range of 10–60° with the scan step of 0.02°. The phase analysis, quantitative analysis and lattice parameters calculations were made by using the PDXL2 software on the Rigaku's system.

A 0.64 m focal length single grating (600 mm^{-1}) monochromator and the 442 nm line of a He–Cd laser with different power were used for the photoluminescence measurements. A closed-cycle helium cryostat was employed to measure temperature dependencies of the PL spectra and reflectivity at temperatures from 10 K to 300 K. A stabilized 300 W halogen lamp was used in reflectivity measurements. The Hamamatsu InGaAs PMT detector using digital lock-in technique detected optical signals.

3. Results and discussion

3.1. XRD studies

The synthesized CCGSe powder and single crystals were first analyzed by XRD, see figure 1.

According to this study both samples contain about 89% of CCGSe with an orthorhombic structure (*Pmn*21) with lattice parameters $a = 8.061$ Å, $b = 6.871$ Å, $c = 6.599$ Å, and about 11% of CCGSe with a tetragonal structure (*I*-42*m*) with lattice parameters $a = b = 5.750$ Å, $c = 11.049$ Å. These values are similar to lattice parameters found in [4, 5, 7].

3.2. Laser power dependence and reflectivity measurements

Low-temperature PL spectra of polycrystalline sample showed an asymmetric band with peak position at about 1.17 eV, see figure 2(a).

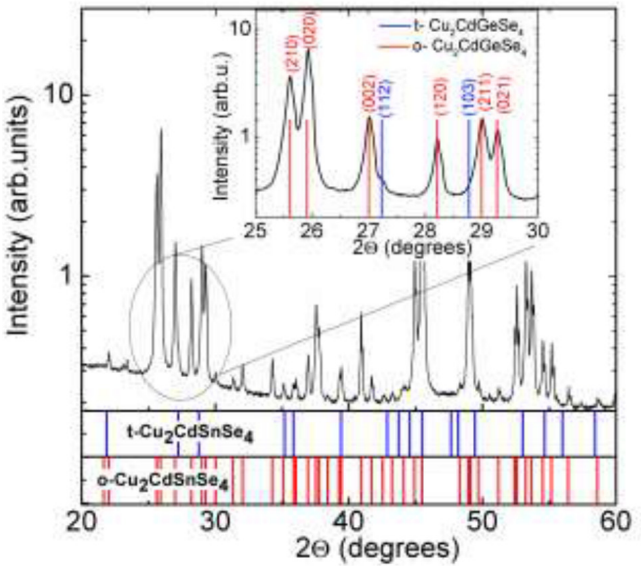

Figure 1. XRD pattern of CCGSe polycrystals. The inset shows a most interesting region, where the presence of tetragonal phase can be detected. The XRD patterns of standard orthorhombic and tetragonal structures of CCGSe are also shown.

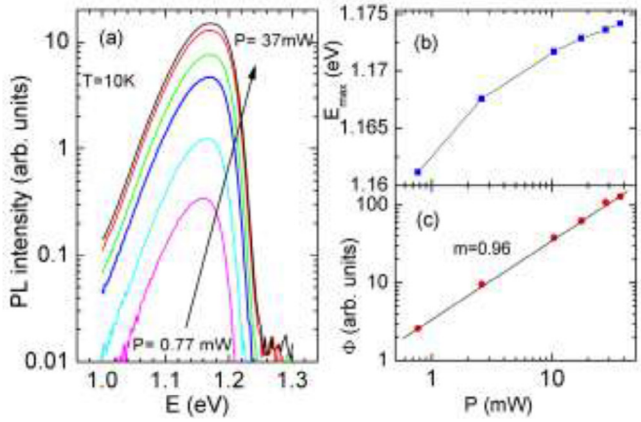

Figure 2. (a) Excitation intensity dependence of PL spectra of polycrystalline $Cu_2CdGeSe_4$ sample measured at $T = 10$ K, (b) the peak position shift and (c) the integral intensity Φ of the PL band on laser power.

Our previous study revealed 2 PL bands at 1.218 eV and 1.146 eV in the o-CCGSe and one PL band at 1.053 eV in the t-CCGSe [7]. The presence of only one PL band in our current samples allows a more detailed study of the PL band shape. It can be seen from figure 2(c) that the integrated intensity Φ (P) of PL band depends on the excitation laser power P as $\Phi \sim P^m$. The power coefficient m can be found as the gradient of the Φ (P) plot on a log-log scale as shown in figure 2(c) giving a value $m = 0.96$ for the studied PL band. Radiative recombination of charge carriers localized at defects with energy levels below the band gap is assigned for m values smaller than unity [14] and therefore we expect that the observed PL band is mostly associated with recombination involving defect levels within the bandgap. Figure 2(b) demonstrates that the PL band blueshifts with increasing laser power to higher energies, the shift being smaller at higher laser powers. The overall shift is less than 7 meV per decade of laser power. At the same time

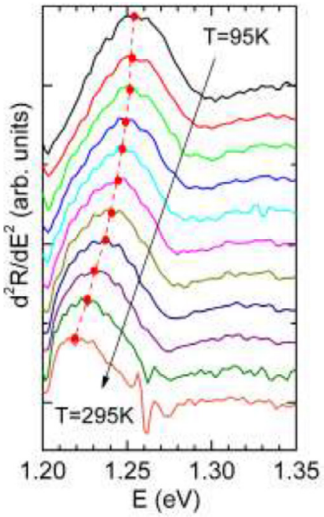

Figure 3. Temperature dependence of 2nd derivative of reflectivity R measured from the $Cu_2CdGeSe_4$ single crystal sample.

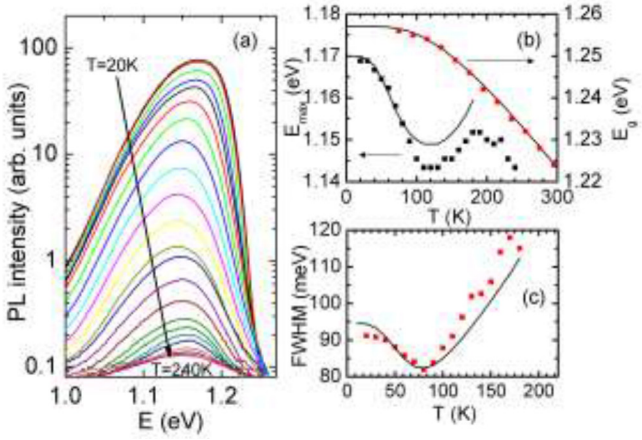

Figure 4. (a) Temperature dependent PL spectra of polycrystalline $Cu_2CdGeSe_4$ sample, (b) the temperature dependence of the peak position E_{max} (experimental data-dots, calculated dependence-solid line) and the band gap energy E_g (experimental data- dots, fitting result with equation (1)—solid line) and (c) FWHM (experimental data-dots, calculated dependence-solid line).

both, the low energy side and the high energy side of the band show the same unchanged shape and the only effect of the laser power increase is related to the continuous blueshift of the high energy side and thus, widening of the PL band.

Results of reflectivity R measurements of the CCGSe single crystal at different temperatures are presented in figure 3.

It is known, that reflectivity spectrum is usually very sensitive to critical points in the band structure and all these features are more pronounced in the second derivative d^2R/dE^2 spectra, where the maximum corresponds to the band gap energy Eg [15]. Figure 3 shows a temperature dependent second derivative reflectivity spectra measured in the temperature range $T = 95$–295 K. The peak maximum of these spectra corresponds to a band gap energy E_g. The temperature dependence of the band gap energy found from figure 3 is plotted in figure 4(b).

Unfortunately, at very low temperatures we could not get reliable reflectivity signal. The temperature dependencies of

E_g were fitted with the expression introduced by O'Donnell and Chen [16]:

$$E_g(T) = E_g(0) - S\langle\hbar\omega\rangle / [\coth(\langle\hbar\omega\rangle/2kT) - 1], \quad (1)$$

where $E_g(0)$ is the band gap energy at 0 K, S is a dimensionless coupling constant and $\langle\hbar\omega\rangle$ represents an average phonon energy. The solid curve in figure 4(b) is the best fit with parameters: $E_g(0) = 1.257$ eV; $S = 1.35$; $\langle\hbar\omega\rangle = 34$ meV. This average phonon energy is very close to the highest Raman mode detected in o-CCGSe at 277 cm^{-1} (34.3 meV) [4] and probably corresponds to the LO-phonon. The room temperature band gap energy in our CCGSe ($Eg = 1.223$ eV) is slightly less than the reported value of the band gap energy in pure orthorhombic CCGSe ($E_g = 1.27$ eV) [4] and this difference is most likely due to the mixing with a tetragonal phase. According to figure 4(b) the peak position of the PL band at $T = 10$ K is at about 85 meV lower energy than the E_g. This could be an additional proof that a deep defect level is contributing to the recombination process.

3.3. Temperature dependence of PL emission and carrier localization model

The asymmetric shape of the PL band is typical for disordered systems, where different fluctuations can affect the shape of DOS function. Both, valence and conduction band edges are usually affected. In case of deeper defect levels fluctuations can disturb also these levels and, as a result, defect band is formed instead of discrete level. As a rule, the low energy side of these asymmetric PL bands at low temperatures is more or less determined by the DOS function $\rho(E)$ while the Fermi distribution function $f(E)$ controls the shape of the high energy side of the PL band [9]. In ternary copper chalcogenides, where the high concentration of charged defects creates spatial electrostatic potential fluctuations, the low energy side of PL bands has often an exponential shape [17], but the Gaussian shape is also detected [18]. In general, the increase of measurement temperature leads to widening of the high energy side of PL bands while the width of the low energy side remains almost unaffected [19]. As a result, a continuous increase of the full width at half maximum (FWHM) of the PL band with temperature is observed. The temperature dependence of the PL band in our CCGSe sample is presented in figure 4(a). The low energy side of the band shows a Gaussian shape and the peak position has a 'S-shaped' behavior with temperature. At the same time, the FWHM has a 'V-shaped' dependence characteristic for localized states, see figure 4(c).

All measured asymmetric PL spectra were fitted similarly to [20] using a following simplified function:

$$I(E) \propto \rho(E) f(E) \propto \exp\left[-\frac{(E-E_0)^2}{2\gamma^2}\right] * \frac{1}{\exp\left(\frac{E-E_F^*}{kT^*}\right)}, \quad (2)$$

where E_0 is a peak position and γ is a width of DOS, E_F^* is a quasi Fermi level position and T^* is an effective carrier temperature. γ can be considered as an average amplitude of fluctuations. From the fitting of the experimental PL spectrum with

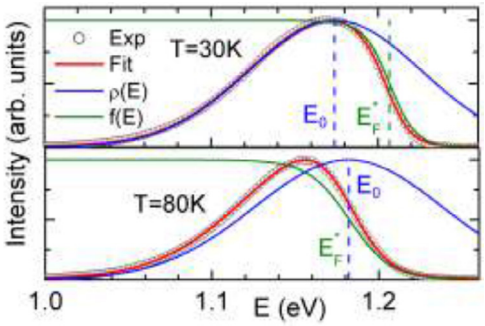

Figure 5. Example of curve fitting using equation (2) for two different temperatures. Open dots represent measured spectra, red solid lines show the general fitting result while green and blue lines are $f(E)$ and $\rho(E)$, respectively. All curves are normalized.

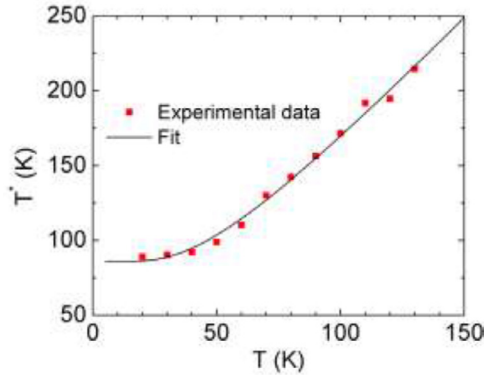

Figure 6. Temperature dependence of extracted effective carrier temperature T^* obtained from PL band shape fittings (dots). Fitting result using equation (3) is shown as a continuous line.

equation (2) we get $\gamma = 50$ meV at $T = 10$ K. The equation (2) represents a normalized shape and must be multiplied with the intensity value. Few examples of the curve fitting are presented in figure 5. All measured PL spectra can be well fitted using this model in the temperature range $T = 10$–180 K. At higher temperatures the DOS function becomes more complex and the fitting with equation (2) is not possible. As shown in figure 5, at lower temperatures, the high energy side of the PL band is definitely determined by the Fermi function, but in order to satisfy the actual shape of the band, the carrier temperature $T^* > T$ must be used.

Although, in principle, the carrier temperature could be extracted from the shape of the PL band, increasing the lattice temperature also results in phonon-related broadening of the PL spectra. Therefore, the extracted carrier temperature from PL spectra is usually slightly higher than the real carrier temperature and the difference is greater at higher temperatures. Accordingly, the term 'effective carrier temperature' is used here. The temperature dependence of effective carrier temperature T^* can be fitted using a simple empirical equation:

$$T^*(T) = T_0^* + a_1 / [\exp(a_2/kT) - 1], \quad (3)$$

where $T_0^* = 86$ K, $a_1 = 231$ K and $a_2 = 11.4$ meV, see figure 6.

Here we assume, that the lattice temperature is identical to measurement temperature T. Even at $T = 10$ K we have hot carriers with a temperature about 75 K higher than the lattice

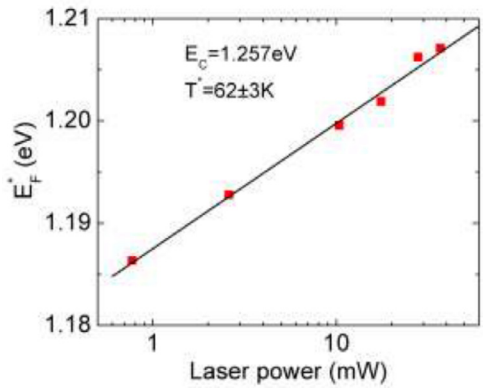

Figure 7. Experimentally determined position of quasi Fermi level on laser power at $T = 10$ K. Fitting using equation (4) is given as a solid line.

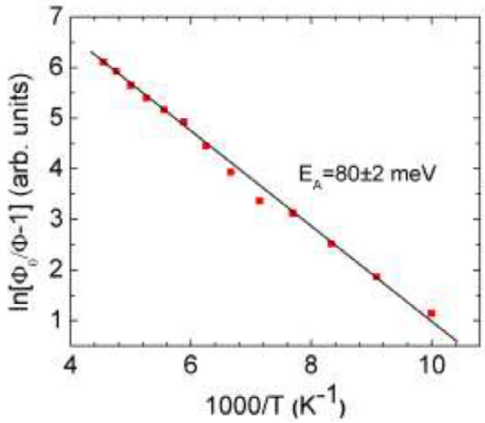

Figure 8. Temperature dependence of integral intensity (dots) of PL band and a fitting results with equation (5) (line). The thermal activation energy of acceptor defect is $E_A = 80$ meV.

temperature. For higher lattice temperatures ($T > 60$ K), the dependence of the hot carriers temperature on the lattice temperature is nearly linear to a good approximation. Similar behavior was detected also in other materials like PbS quantum dots [21], in GaSb-based multi quantum wells [22], in $GaAs_{1-x}N_x$ [23], and in Si [24]. Hot carriers would usually quickly undergo carrier-phonon (mostly LO-phonons) interaction and release the excess energy above the bandgap as lattice vibration through emission of phonons on the order of picoseconds. In a steady-state photoluminescence, however, the equilibrium between carrier thermalization, recombination and excitation processes will be achieved. The lattice temperature has a large impact on the thermalization rate of the carriers. This is because the lattice temperature change could influence the occupation number of the phonon modes involved in the process and hence affects the hot phonon lifetime. The increasing difference $T^* - T$ with increasing lattice temperature indicates to the decreasing of cooling efficiency of hot carriers at elevated lattice temperatures.

As it was depicted in figure 2, the high-energy side of the PL band showed a continuous blueshift with increasing laser power. According to our model this shift can be explained as a variation of the quasi Fermi level position E_F^*. We propose that the position of the electron quasi Fermi level can be calculated using a classical approach:

$$E_F^* = E_C - kT^* \ln[\frac{N_C}{n}] \tag{4}$$

where E_C is an energetic position of conduction band edge, T^* is an effective carrier temperature, N_C is an effective DOS of the conduction band and the concentration of electrons n depends linearly on the laser power P: $n \sim P$. Figure 7 shows the dependence of experimentally determined E_F^* values on laser power at $T = 10$ K together with the fitting result with equation (4).

The best fitting was achieved with $E_C = E_g = 1.257$ eV and with effective carrier temperature $T^* = 62$ K. This is slightly lower than the temperature determined from the shape of PL band. However, this result shows that the blueshift of the PL band with increasing laser power is related to the state filling effect. Very similar dependence of the PL band shape on laser power was also observed recently in CZTSSe [25].

The temperature dependence of the integral intensity Φ of the PL band is presented in figure 8.

The PL peak integral intensity decreases with temperature according to the simple exponential law [26]:

$$\Phi(T) = \Phi_0 / \left[1 + \alpha \exp\left(\frac{E_A}{kT}\right)\right], \tag{5}$$

where Φ_0 is a PL intensity at $T = 0$ K, α is a process rate parameter and E_A is a thermal activation energy. When plotted in coordinates such as used in figure 8, one should have a straight line and from its slope the thermal activation energy E_A can be calculated. In our case the activation energy $E_A = 80 \pm 2$ meV was obtained from the fitting. This thermal activation energy is nearly identical to the separation of the PL band peak position from the band gap energy E_g, see figure 4(b). Therefore, it is reasonable to believe that the PL band is related to the radiative recombination of electrons with holes captured by the acceptor level having a depth $E_A = 80 \pm 2$ meV. The thermal quenching of the PL band at higher temperatures is a result of ionization of this rather deep acceptor level. However, experimentally observed dependences do not confirm this simple model. The 'S-shaped' behavior of the peak position and especially the 'V-shaped' behavior of the FWHM with temperature, see figures 4(b) and (c), are typical for photoluminescence related to localized carriers and their redistribution between potential wells with different depth [27]. In principle, in p-type compounds electrons are able to localize inside local potential wells created by high concentration of charged donor defects if there is a sufficient large number of donors forming a charged donor clusters [9]. In this case so-called TT (tail to tail) and TI (tail to deep acceptor level) transitions could be possible. However, these electrostatic potential fluctuations affect also acceptor levels and the recombination probability will depend on an electron-hole separation like in case of donor-acceptor pairs. Therefore, at low temperatures, when holes cannot approach donor clusters, the PL intensity should drop. We did not see any decrease of the PL intensity at low temperatures and therefore we exclude these possible recombinations related to donor clusters. Moreover, due to very small effective mass and due to small radius of potential wells created by electrostatic

potential fluctuations in so-called 'heavily doped' materials, electrons are not able to localize inside of these rather small regions with a radius $r \approx N_D^{-1/3}$, where N_D is a concentration of donor defects. The situation is different with more heavier holes and therefore so-called band to tail emission, where holes are localized within potential wells deep in valence band tail, is so common in ternary copper chalcogenides [19]. But electrons can localize in potential wells with slightly larger width created by fluctuations of the band gap energy due to a presence of different phases with different E_g, lateral spatial variations of composition or strain [10]. Recently this concept was also demonstrated in WS_2 monolayers, where band gap energy fluctuations were caused by random distribution of local tensile strain [27]. But these random Gaussian band gap fluctuations are quite common also in solid solutions of semiconductors [12] or in compounds where different crystal modifications with different band gap energy are present. In our samples we have a mixture of orthorhombic ($Pmn2_1$) and tetragonal (I-42m) structures with band gap energies 1.27 eV and 1.14 eV, respectively [4]. A random distribution of the tetragonal phase with a smaller band gap energy then causes these Gaussian band gap energy fluctuations. The average depth of band gap fluctuations γ_B can be estimated from the peak position shift with increasing temperature. According to figure 4(b) this shift is around 30 meV. At the same time the overall average depth of fluctuations γ determined from the PL band shape was significantly higher. This difference can be explained by the additional effect of spatial electrostatic potential fluctuations with average depth of γ_E. Then, as was proposed in [28], the total depth of fluctuations is a combination of both fluctuations: $\gamma = (\gamma_B^2 + \gamma_E^2)^{1/2}$ and, by assuming that $\gamma = 50$ meV, we get a value $\gamma_E \approx 40$ meV. Very similar situation with co-occurrence of electrostatic and band gap fluctuations was seen also in $CuGa_3Se_5$ [29]. As it was mentioned earlier, electrons are not able to localize inside of small range potential wells created by spatial electrostatic potential, but holes at deep acceptor levels are affected by these fluctuations and, as a result, the DOS function will broaden. The $\rho(E)$ function in our case represents a specific mixture of electron and hole states, where electron states are affected only by band gap fluctuations and hole states are additionally affected by electrostatic potential fluctuations.

At very low temperatures optically generated electrons are trapped by nearby shallow local potential minima close to E_c. The quasi Fermi level is also at its highest position. When the temperature increases, electrons from these shallow states start to migrate into deeper minima, where the tetragonal structure with a smaller E_g is dominating and the E_F^* level decreases accordingly. This process leads to a sharp redshift of a PL band peak position with temperature and the FWHM will also decrease due to a redshift of E_F^*. The redistribution of electrons between shallow and deep potential wells is possible when the size of these wells is in the same range as the minority carriers diffusion length [10]. It is important that the rate of the peak position redshift did not change with decreasing laser power and the same behavior was observed also in CZTSSe [25]. In ternary chalcogenides, where spatial potential fluctuations are dominating, the rate of the redshift increases with decreasing the laser power [9]. Starting from temperatures $T = 110$–120 K electrons are able to delocalize from these deeper potential wells and electrons start to occupy states with $E \geqslant E_c$. Therefore, the peak position shows a blueshift with temperature and from $T \approx 180$ K it starts to follow the temperature dependence of E_g. The temperature dependence of the quasi Fermi level shows a complex behavior, because starting from temperature $T \approx 100$ K the thermal energy is already sufficient to exponentially increase the concentration of electrons and therefore, according to equation (4), the shift of E_F^* with increasing temperature starts to slow down. The peak position of DOS (E_0) shows a weak temperature dependence, but at $T > 130$ K, when conduction band states start to contribute, a rapid shift towards higher energies is observed.

We also tried to calculate, using equation (2), the temperature dependence of peak position and FWHM taking into account all above mentioned temperature dependences of E_g, T^*, E_F^*, n, and E_0. In addition, the widening of DOS due to electron–phonon interaction [30], i.e. $\gamma = \gamma_0 + \Gamma/[\exp(\hbar\omega_{LO}/kT) - 1]$ with LO-phonon energy $\hbar\omega_{LO} = 34$ meV found from the temperature dependence of E_g was taken into account. Results of these calculations are presented in figures 4(b) and (c) as solid lines. Although temperature dependences for important parameters are more like estimation, the calculated temperature dependences of the characteristic parameters are in good collelation with the experimental data.

In kesterite compounds like CZTSe and CZTS the dominating Cu_{Zn} acceptor defect has an activation energy close to 100 meV [31]. Photoluminescence properties and the depth of potential fluctuations of the studied sample are quite similar to kesterite compounds and therefore the Cu_{Cd} acceptor could be also the most probable defect causing the radiative recombination in our CCGSe. But this hypothesis must be tested in future experiments.

It is known that small-scale electrostatic potential fluctuations are very harmful for every absorber material used in solar cells because they lead to a decrease of the device efficiency. In contrast, the band gap energy fluctuations have much wider scale. However, both fluctuations should be avoided and therefore more studies are needed to prevent the formation of different phases and band gap energy fluctuations in CCGSe.

4. Conclusions

In summary, we investigated the radiative recombination mechanism in the polycrystalline $Cu_2CdGeSe_4$ over the excitation power range of 0.77 to 37 mW and the temperature range of 10 to 300 K. XRD analysis revealed the presence of 89% of the orthorhombic and 11% of the tetragonal phase in the studied sample. Observed 'S-shaped' and 'V-shaped' temperature dependences of the emission energy and linewidth, respectively, are typical for recombination including localized carriers and their redistribution between potential wells with different depth. It was shown that electrons are localized in potential wells created by random band gap energy fluctuations having a Gaussian shaped DOS function while holes are localized at acceptor states created probably by Cu_{Cd} acceptor defect with a depth of 80 meV. The asymmetric PL band shape

analysis indicates the presence of hot carriers with a temperature about 75 K higher than the lattice temperature. The band gap energy fluctuations are caused by a small fraction of tetragonal phase having a smaller band gap energy. In addition to band gap energy fluctuations, electrostatic potential fluctuations with an average depth of 40 meV were also present.

Acknowledgments

This work was supported by institutional research fundings IUT (IUT19-28, IUT19-4) of the Estonian Ministry of Education and Research and by the European Union through the European Regional Development Fund, Project TK141.

ORCID iDs

Jüri Krustok https://orcid.org/0000-0002-4671-2332

References

[1] Wang W, Winkler M T, Gunawan O, Gokmen T, Todorov T K, Zhu Y and Mitzi D B 2014 Device characteristics of CZTSSe thin-film solar cells with 12.6% efficiency *Adv. Energy Mater.* **4** 1301465

[2] Gulay L D and Parasyuk O V 2002 Crystal structures of low- and high-temperature modifications of $Cu_2CdGeSe_4$ *J. Alloys Compd.* **347** 193–7

[3] Brik M G, Parasyuk O V, Myronchuk G L and Kityk I V 2014 Specific features of band structure and optical anisotropy of $Cu_2CdGeSe_4$ quaternary compounds *Mater. Chem. Phys.* **147** 155–61

[4] Kauk-Kuusik M *et al* 2018 Study of $Cu_2CdGeSe_4$ monograin powders synthesized by molten salt method for photovoltaic applications *Thin Solid Films* **666** 15–9

[5] Matsushita H, Ichikawa T and Katsui A 2005 Structural, thermodynamical and optical properties of Cu_2-II-IV-VI_4 quaternary compounds *J. Mater. Sci.* **40** 2003–5

[6] Chetty R, Dadda J, de Boor J, Müller E and Mallik R C 2015 The effect of Cu addition on the thermoelectric properties of $Cu_2CdGeSe_4$ *Intermetallics* **57** 156–62

[7] Grossberg M, Raadik T, Krustok J, Kauk-Kuusik M, Timmo K, Kaupmees R, Mikli V and Mere A 2018 Optical and structural properties of orthorhombic and tetragonal polymorphs of $Cu_2CdGeSe_4$ *Thin Solid Films* **666** 44–7

[8] Gokmen T, Gunawan O, Todorov T K and Mitzi D B 2013 Band tailing and efficiency limitation in kesterite solar cells *Appl. Phys. Lett.* **103** 103506

[9] Levanyuk A P and Osipov V V 1981 Edge luminescence of direct-gap semiconductors *Sov. Phys. Usp.* **24** 187–215

[10] Mattheis J, Rau U and Werner J H 2007 Light absorption and emission in semiconductors with band gap fluctuations—a study on Cu(In,Ga)Se_2 thin films *J. Appl. Phys.* **101** 113519

[11] Rey G, Redinger A, Sendler J, Weiss T P, Thevenin M, Guennou M, El Adib B and Siebentritt S 2014 The band gap of $Cu_2ZnSnSe_4$: effect of order-disorder *Appl. Phys. Lett.* **105** 112106

[12] Lourenço S A, Dias I F L, Duarte J L, Laureto E, Aquino V M and Harmand J C 2007 Temperature-dependent photoluminescence spectra of GaAsSb/AlGaAs and GaAsSbN/GaAs single quantum wells under different excitation intensities *Brazilian J. Phys.* **37** 1212–9

[13] Li Q, Xu S J, Xie M H and Tong S Y 2005 A model for steady-state luminescence of localized-state ensemble *Europhys. Lett.* **71** 994–1000

[14] Schmidt T and Lischka K 1992 Excitation power dependence of the near-bandgap-edge photoluminescence of semiconductors *Phys. Rev.* B **45** 8989–94

[15] Guc M, Levcenko S, Dermenji L, Gurieva G, Schorr S, Syrbu N N and Arushanov E 2014 Exciton spectra and energy band structure of $Cu_2ZnSiSe_4$ *J. Alloys Compd.* **587** 393–7

[16] O'Donnell K P and Chen X 1991 Temperature dependence of semiconductor band gaps *Appl. Phys. Lett.* **58** 2924–6

[17] Krustok J, Raudoja J, Yakushev M, Pilkington R D and Collan H 1999 On the shape of the close-to-bandedge photoluminescent emission spectrum in compensated $CuGaSe_2$ *Phys. Status Solidi* **173** 483–90

[18] Siebentritt S, Papathanasiou N and Lux-Steiner M C 2006 Potential fluctuations in compensated chalcopyrites *Physica* B **376–7** 831–3

[19] Krustok J, Collan H, Yakushev M and Hjelt K 1999 The role of spatial potential fluctuations in the shape of the PL bands of multinary semiconductor compounds *Phys. Scr.* **T79** 179

[20] Krustok J, Kaupmees R, Jaaniso R, Kiisk V, Sildos I, Li B and Gong Y 2017 Local strain-induced band gap fluctuations and exciton localization in aged WS_2 monolayers *AIP Adv.* **7** 065005

[21] Cao W *et al* 2016 Quantification of hot carrier thermalization in PbS colloidal quantum dots by power and temperature dependent photoluminescence spectroscopy *RSC Adv.* **6** 90846–55

[22] Le Bris A, Lombez L, Laribi S, Boissier G, Christol P and Guillemoles J-F 2012 Thermalisation rate study of GaSb-based heterostructures by continuous wave photoluminescence and their potential as hot carrier solar cell absorbers *Energy Environ. Sci.* **5** 6225

[23] Bhuyan S, Das S K, Dhar S, Pal B and Bansal B 2014 Optical density of states in ultradilute GaAsN alloy: coexistence of free excitons and impurity band of localized and delocalized states *J. Appl. Phys.* **116** 023103

[24] Boukhatem M H, El Tahchi M, El Haj Moussa G W, Ajaka M, Khoury A and Mialhe P 2007 Carriers temperature for an operating silicon p–n junction *Microelectron. J.* **38** 615–9

[25] Lang M, Zimmermann C, Krämmer C, Renz T, Huber C, Kalt H and Hetterich M 2017 Luminescence properties of $Cu_2ZnSn(SSe)_4$ solar cell absorbers: state filling versus screening of electrostatic potential fluctuations *Phys. Rev.* B **95** 155202

[26] Krustok J, Collan H and Hjelt K 1997 Does the low-temperature arrhenius plot of the photoluminescence intensity in CdTe point towards an erroneous activation energy? *J. Appl. Phys.* **81** 1442–5

[27] Wang H, Ji Z, Qu S, Wang G, Jiang Y, Liu B, Xu X and Mino H 2012 Influence of excitation power and temperature on photoluminescence in InGaN/GaN multiple quantum wells *Opt. Express* **20** 3932

[28] Werner J H, Mattheis J and Rau U 2005 Efficiency limitations of polycrystalline thin film solar cells: case of Cu(In,Ga)Se_2 *Thin Solid Films* **480–1** 399–409

[29] Grossberg M, Krustok J, Jagomägi A, Leon M, Arushanov E, Nateprov A and Bodnar I 2007 Investigation of potential and compositional fluctuations in $CuGa_3Se_5$ crystals using photoluminescence spectroscopy *Thin Solid Films* **515** 6204–7

[30] Rudin S and Reinecke T L 1990 Temperature-dependent exciton linewidths in semiconductor quantum wells *Phys. Rev.* B **41** 3017–27

[31] Chen S, Walsh A, Gong X-G and Wei S-H 2013 Classification of lattice defects in the kesterite Cu_2ZnSnS_4 and $Cu_2ZnSnSe_4$ earth-abundant solar cell absorbers *Adv. Mater.* **25** 1522–39